



Assessment of Stability Conditions of Ancient Underground Quarries using On-Site Monitoring and Numerical Modeling

Anna Maria Ferrero, Professor, Dept. of Civil and Environmental Engineering and Architecture, University of Parma, Parma, Italy; e-mail: annamaria.ferrero@unipr.it

Andrea Segalini, Professor, Dept. of Civil and Environmental Engineering and Architecture, University of Parma, Parma, Italy; e-mail: andrea.segalini@unipr.it

ABSTRACT: *This work, carried out by members of the University of Parma's Department of Civil and Environmental Engineering and Architecture, analyzes the stability of the ancient underground quarries at Viggìù (Varese, Italy). The objective of the study was to verify the actual structural predisposition to instability phenomena in the ancient ornamental stone quarries for a historical and cultural valorization as well as the recovery of the Danzi and Beltrami quarries. Although completely abandoned, these sites could be used as a tourist attraction and/or as a teaching environment. They are a wonderful example of industrial architecture, presenting audacious compositions of filled-in trenches and room and pillar techniques (Hedley and Grant, 1972). With such objectives in mind, a monitoring system that aims to control the most significant joints and discontinuities of the site has been realized. A numerical model of the entire rock mass has been developed in order to analyze the stability of the underground openings. A route for visitors has also been identified.*

KEYWORDS: Stability, underground quarries, monitoring, numerical modeling

SITE LOCATION: [IJGCH-database.kmz](#) (requires Google Earth)

INTRODUCTION

The objective of this study was to consider the structural instability of the rock mass at the Viggìù ancient underground quarries (Varese province, Italy). The aim was to achieve a complete historical and cultural restoration of the Danzi and Beltrami quarries. The monitoring system that was installed allows for the continuous control of the rock mass deformation and provides an immediate evaluation of its evolution over time. The system has a dual function: the first is to acquire preliminary data that would allow for the calibration of the rock mass numerical model; the second is the control of potential instability—particularly when the quarry complex will be opened to the public. This second phase would require the setting up of an automatically controlled alarm system that could be constantly updated. Both the numerical simulation of the natural and induced state of stress and the provisional numerical model have been supported by on-site and laboratory tests and have been developed in order to retrofit the monitoring system with the data they acquire. The study, which started from the geological and geomorphological overview of the surroundings of the site through historical records and observation of the current state of these ancient quarries, deals with the morphological and structural characterization of the mined areas (such as the discontinuities, karst, pillars, entrances, etc.) and with the theoretical aspects of rock mass geostructural surveys. All of these aspects are considered in order to define the automatic monitoring of displacements and the control system and to choose the main discontinuities to be monitored as well as the most appropriate hardware and software instrumentation. The data recovered by the monitoring system are graphically presented, highlighting the actual movements and their periodic variation. Finally, this study considers the evolution of the disturbed zone around the underground openings when some fundamental features of the rock mass (cohesion and friction angle of joints and matrix and original state of stress) can be modified by rock weathering. The results are interpreted in light of a strong relationship between the rock mass characteristics and the stability of the underground opening. Numerical modeling techniques were extensively used, starting from the geometrical reconstruction of the fractured rock mass, passing through the identification, reconstruction and stability analysis of complex rock blocks using the ROCK3D (Geo&Soft, 2008) calculation code, and arriving at the formulation of a complete finite element method (FEM) model of the entire area using the ABAQUS® code

Submitted: 17 October 2010; Published: 10 March 2011

Reference: Ferrero, A.M., and Segalini, A., (2011). *Assessment of Stability Conditions of Ancient Underground Quarries using On-Site Monitoring and Numerical Modeling*. International Journal of Geotechnical Engineering Case Histories, <http://casehistories.geoengineer.org>, Vol.2, Issue 1, p.66-85. doi: 10.4417/IJGCH-02-01-04.



(Hibbit, Karlsson and Sorensen, Inc., 1994).

GEOGRAPHICAL, GEOLOGICAL AND GEOMORPHOLOGICAL SETTING

The studied area underlies a surface of approximately 15 km², distributed between the communities of Arcisate, Bisuschio, Clivio, Saltrio, and Viggìu in the province of Varese, Italy.

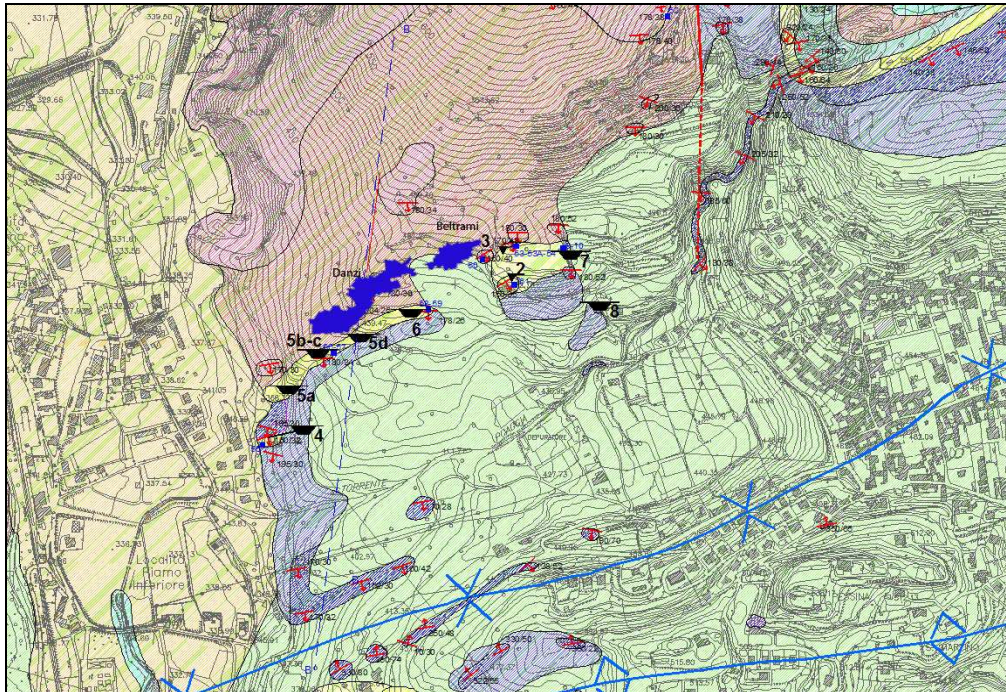


Figure 1. Geological map of area (reproduced from Scesi, 2000), with indication of section B–B' (see Figure 2) and area occupied by underground quarries (solid blue). See legend in Table 1.

The studied sector (see Figure 1) belongs, from geological point of view, to the Alpi Meridionali (Sudalpino) tectonic unit, more precisely located within the western portion of the Prealpi Lombarde (Scesi, 2000). The unit is formed by a series of tectonic flakes that, due to the compressive tectonic movements connected with the beginning of the closure of the Ligurian–Piedmont Basin, are partially overthrust one above the other. Their sliding planes dip irregularly toward the north, producing an apparent orientation to the south of the majority of the tectonic elements. The outcropping rocks that are of a sedimentary nature and have a prevailing carbonitic composition (limestones and dolomite) and siliceous suborder cover a timespan between the Superior Triassic (approx. 230 Million years ago.) and the Inferior Cretaceous periods.

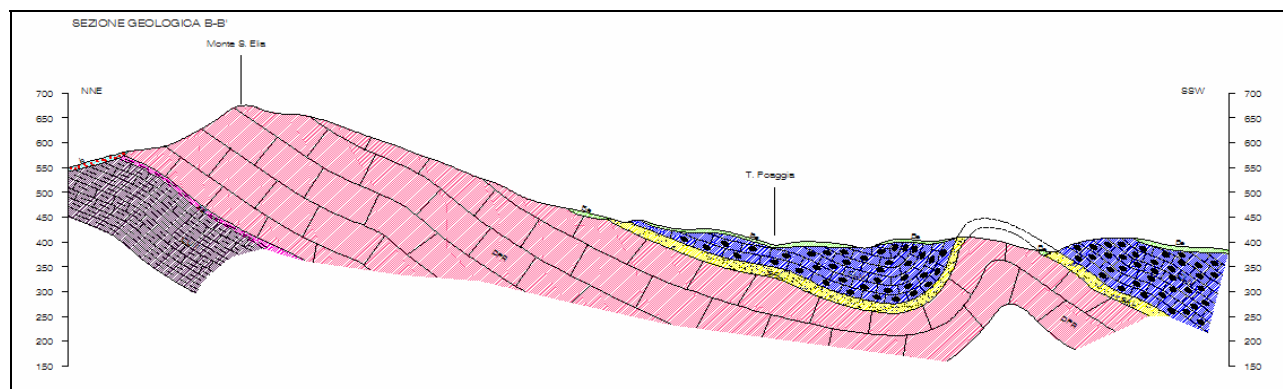
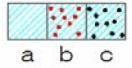





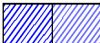




Figure 2. Geological section of area subjected to quarry activities (from Scesi, 2000).



Table 1. Key for Figure 1 and 2 (from Scesi, 2000).

PLIOCENIC – QUATERNARY DEPOSITS	
	Post-glacial unit
	Cantu allochthonous formation (Upper Pleistocene)
	Besnate undifferentiated formation (Middle Pleistocene–Upper Pleistocene)
	Mendrisio conglomerates (Upper Pliocene–Upper Pleistocene)
	Saltrio unit (Upper Pliocene–Upper Pleistocene)
	Bevera stock (Upper Pleistocene)
BEDROCK	
	Moltrasio limestone (Middle Lias)
	Saltrio limestone (Lower Lias)
	Primary dolomite (Upper Trias) (Norico)

From a structural geology point of view, the above-mentioned rock masses are organized in a succession of anticlinal and synclinal folds, having their axes with a prevailing averaged direction of E–W or NNE–SSW. These structures are variously dislocated by old structural lineation with a prevailing N–S direction or, in suborder, WSW–ENE that were already present during the distensive phase of the Superior Triassic–Inferior Jurassic. These structural elements have determined the typical paleographic configuration known as horst and graben, and some of them were reactivated during the intermediate and late alpine orogenesis phases. The bedrock is covered by the series of plio-quadernary deposits of continental origin, primarily originated by glaciers and rivers and, in suborder, by lakes that have been frequently altered by human activities.



Figure 3. View of upper entrance of Danzi quarry.



The morphology of the examined area is primarily connected to its structural order, the gravitational action, the different weathering effects on the various lithology, the modeling activity of glaciers and superficial waters and human activity (not negligible). Along the northern ridge of the S. Elia–Orsa–Pravello massif and along the northern side of Mount Useria, the southern dipping of the principal Dolomia strata determined the formation of tall cliffs and/or subvertical scarps. Road blocks frequently detach along such rock slopes due to a particularly unfavorable relative orientation between the surfaces of the discontinuities and the morphology. The process is favored by the erosion induced by several forces (precipitation and runoff waters, freeze–thaw cycles, etc.). The large rock portions and the detached blocks are feeding the debris deposits at the base of the cliffs. The dimension of the various rock elements is a function of the degree of fracturing of the rock mass. Several tension cracks of variable depths (ranging from a few to several meters long and up to a couple of meters wide) are visible. Some of them are filled with rock blocks and/or soil. These elements indicate the presence of slow sliding processes involving relevant portions of the rock mass.

GEOMECHANICAL SURVEY AND DESIGN OF MONITORING SYSTEM

The on-site surveys and the laboratory and on-site tests, carried out at the beginning of this study, aimed to investigate the mechanical characterization of the lithology that was once exploited for ornamental stone. The surveys also considered the detailed geomorphological characterization of the underground openings and of their surroundings, identifying the dumping areas, the retaining walls, the failures (either those localized at the quarry entrances or those involving walls or other structural elements) and the water infiltration and accumulation areas. A structural survey and mapping of the discontinuities observed on walls, roofs, pillars and diaphragms was also carried out, as well as mapping all the visible karst structures (wells, tunnels and karst discontinuities). Finally, the “disturbed” roof portions, pillars and diaphragm were also identified.



Figure 4. View of middle entrance of Beltrami quarry.



From a mechanical point of view, the main features of the rock masses were also recovered by means of geostructural surveys and laboratory tests performed on the rock matrix and representative samples of the discontinuities. The geomechanical survey also included: the hydraulic features of the rock mass, an analysis of the mechanism of underground water infiltration and circulation, and the areas of infiltration and accumulation that were mapped with an estimate of the inflow–outflow balance.

Table 2 reports the rock matrix mechanical features obtained by laboratory testing on rock blocks taken in the quarry. The blocks were then cored in three different directions (X, Y and Z in Table 2) in relation to the cleavage direction that was easy to identify on the blocks.

Table 2. Mechanical features of rock matrix averaged along three investigated directions and determined using Hoek-Brown criteria (Hoek et al., 2002).

	m_i (-)	C (MPa)	φ (°)	σ_r (MPa)	σ_c (MPa)
Global	9.03	17.63	47.92	10.44	94.31
X	10.24	15.29	49.27	8.38	85.84
Y	8.21	17.06	46.42	10.68	87.69
Z	15.47	14.89	54.73	6.40	99.08

Uniaxial, triaxial and tensile tests were performed. These tests showed that the rock material is characterized by a strong anisotropy due to the presence of cleavage. In order to consider this aspect, the obtained results have been treated separately for three conjugate directions and three different failure envelopes were obtained based on the Hoek-Brown criteria.

The envelopes are curves and thus, for the stability analysis, they were linearized within the range of the normal stress to which the rock mass is subjected. For safety reasons, the lowest of the three computed strength values was then chosen since the cleavage direction was not always clearly identifiable in the real in situ structures.

Direct shear tests on natural discontinuities allowed for the evaluation of the peak and residual strength of natural discontinuities. A peak and residual failure envelope of the discontinuities was achieved with direct shear laboratory tests. The peak and residual angles are 54° and 41°, respectively.

The geomechanical characterization of the rock mass required the execution of scan lines for a survey of discontinuities on the outcropping rocks. All the discontinuities intercepting the scan lines were recorded, and the orientation (dip and dip direction angle), spacing, persistence, wall strength, roughness, aperture, possible filling thickness and presence of water were evaluated for each discontinuity according to the methods suggested by the ISRM (International Society of Rock Mechanics). Orientation data are reported in Table 3. The interpretation of the discontinuity survey allowed for the identification of five discontinuity systems in the rock mass in addition to a foliation plane. The frequency and spacing values are reported in Table 4.

Table 3. Main joint set orientation.

Sets	Dip	Dip direction
1	74±4	270±30
2	74±10	323±20
3	67±5	25±20
4	32±5	159±12
5	83±5	72±20

The rock mass in the excavation zones, which is considered homogeneous from a geomechanical point of view, was classified on the basis of the scan line surveys of discontinuities and laboratory tests. This allowed for the definition of the quality indexes: rock mass rating (RMR) (Bieniawski, 1973) and Q (Barton et al., 1974).

The indexes required to assess the Q value of the Barton classification are: rock quality designation (RQD), reported in Tables 4 and 5 and calculated using the frequency value reported in Table 5 (Jn, Jr, Ja, Jw, and the stress ratio factor



(SRF)). The indexes represent the number of discontinuity families, the surface roughness, the deterioration and filling of joints, the presence of water, and the SRF, respectively.

Table 4. Frequency and spacing values obtained from discontinuity surveys in two examined sites and used for rock mass classification.

Frequency	fS	fK1	fK2	fK3	fK4	fK5	f global	Spacing (m)
Beltrami quarry	3.2	3.5	2.6	1.9	3.6	1.5	16.6	0.06
Danzi quarry	2.4	2.7	2.5	2.5	1.42		11.8	0.09

Table 5. Values considered in rock mass classification.

	ROD	Jn	Jr	Ja	SRF	Jw	Q
Danzi quarry	75	15	3	1	2.5	1	6

The Q values are 6 for the Danzi quarry and 4.8 for the Beltrami quarry. Considering the strength of the rock mass, the calculated RMR value places the rock mass in the third class, for which Bieniawski (Bieniawski, 1973) suggested cohesion values of 0.2–0.3 MPa and friction angles of 25°–35°. Based on the results of the geomechanical surveys, the areas with the higher predisposition to instability were located. Thus, the most influential discontinuities were selected for monitoring. Immediately after the completion of this preliminary activity, a monitoring system was designed based on the outcomes of the surveys and geomechanical analysis. The system is still in place, continuously recording the normal displacements at several discontinuities. There are 15 linear transducers which are connected to three logging units, needed due to the distances between the various areas being monitored. The logging units were named A, B and C (see Figures 6 and 7); the connected transducers were named An, Bn and Cn, respectively, where n is the progressive number of each transducer connected to the loggers. Transducer set A (four sensors, Figure 7) has been placed near the lower entrance of Danzi quarry; transducer set B (seven sensors, Figure 7) has been located at the higher entrance of the same quarry; transducer set C (four sensors, Figure 6) has been installed at the entrance to Beltrami quarry.

The sets had to be located close to the entrances because the logger needed to be covered by the local wireless phone network. This allows for the remote interrogation of the system and for the regular, remote downloading of the acquired data. The readings are taken every three hours and are automatically uploaded to the central server, located at the University of Parma, once a day.

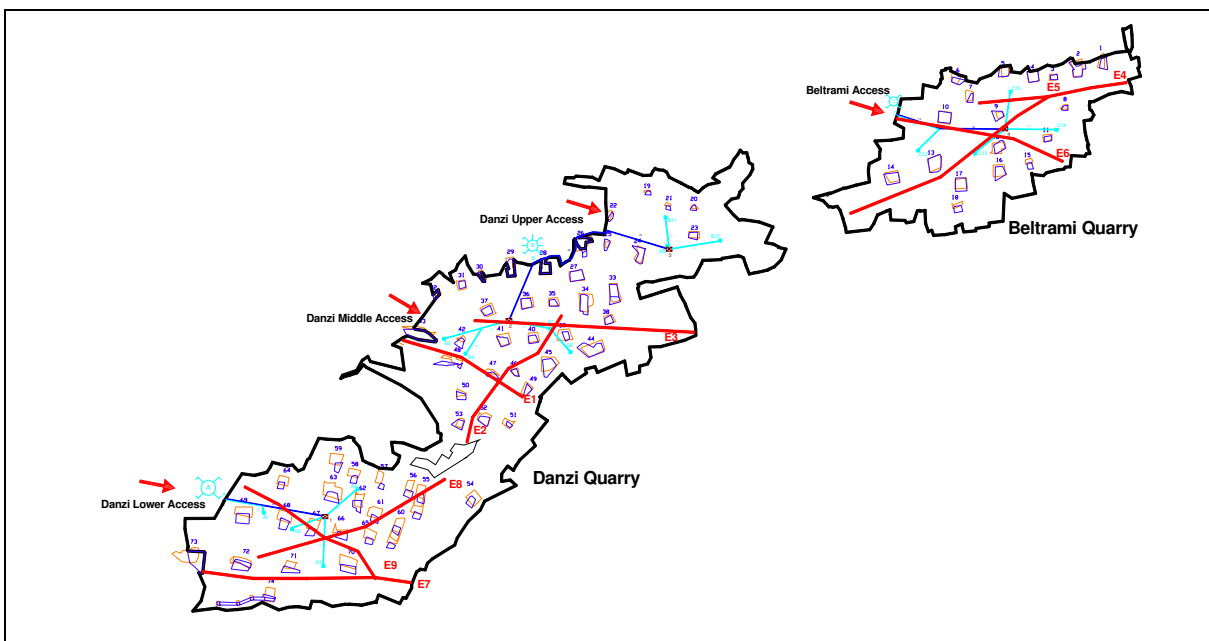


Figure 5. Map of quarries with their names, accesses and respective position. Base (green) and roof (blue) of pillars are numbered and outlined.



The design of the automatic monitoring system is based on the main observed discontinuity features, the installation of the monitoring devices and the initial data verification. The control system is still being refined. Throughout the entire observation period recorded displacements remained within a limit of 0.35 mm when closing and 0.40 mm when opening. During the closing period the average velocity of displacement was about 0.1 mm/month; immediately thereafter a period of opening occurred, displacing 0.75 mm with an average speed of 0.125 mm/month. After this, the displacement tendency switched back to closure, almost completely recovering the registered displacement. Such contractions could probably be explained by the increase in external temperature and the consequent thermal dilation of the rock mass. An example of the trend in the recorded data is reported in Figure 8. Based on the results obtained during the monitoring, the discontinuities appeared to be stable without any increase in aperture or shear displacement.

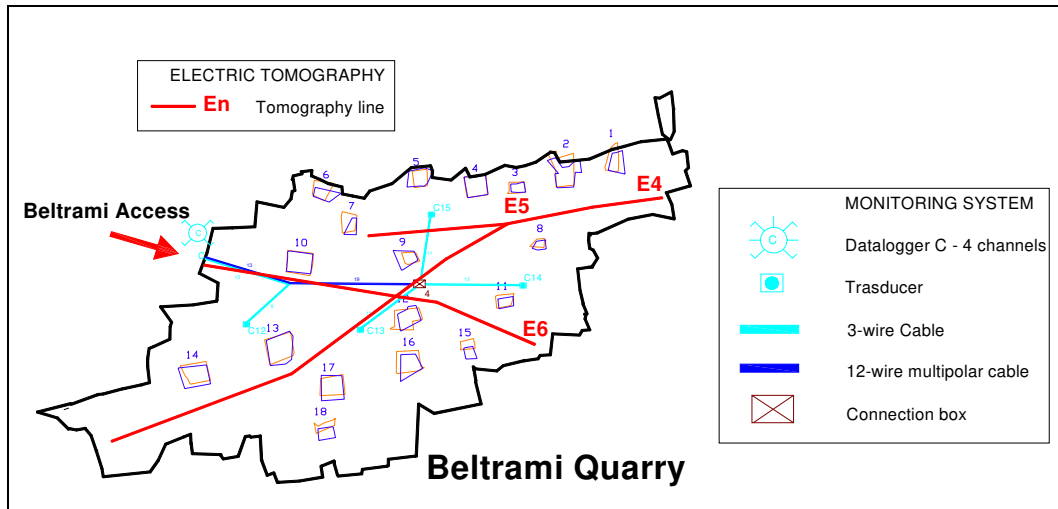


Figure 6. Map of Beltrami quarry showing roofs of pillars (blue) and base (green), monitoring system and tomography lines.

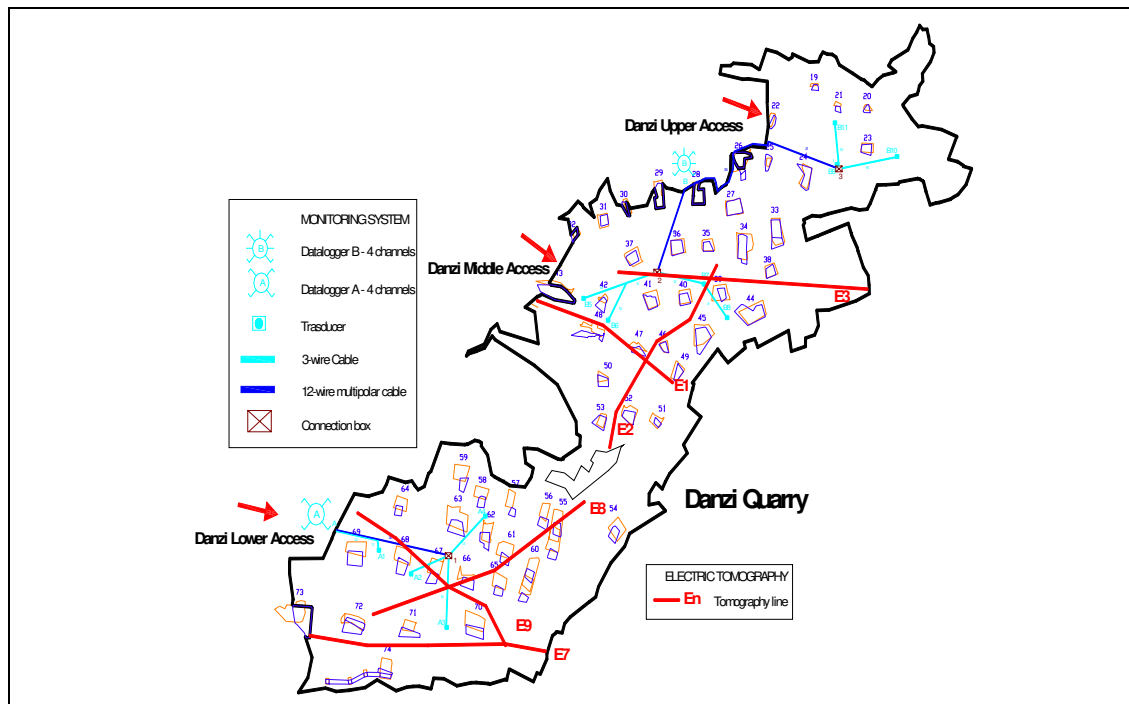


Figure 7. Map of Danzi quarry showing roofs of pillars (blue) and base (green), monitoring system and tomography lines.



On-site Surveys and Tests

Underground Electrical Tomography for Evaluation of Thickness of Excavation Waste Deposits

The analysis aimed to evaluate the thickness of the excavation waste disposal layers that were discharged inside the excavation rooms. The conclusion of mining activity left two features inside the openings. The first is masonry walls of variable height that had been built with discharged rock blocks. These walls serve as retaining walls for the waste material accumulation. The second is wide portions of underground cavities filled with mining waste. Measuring the dimensions of these underground cavities is very difficult to do without the aid of instrumental surveys. The bedrock geometry definition, located at the base of the mining waste accumulation, was carried out using electrical tomography along some predefined lines. That technique was chosen since the expected resistivity contrast between the intact rock and debris was high due to both the presence of a high percentage of voids within the debris and the likely presence of circulating water at the interface. The study of the situation indicated the presence of a continuous and homogeneous debris cover over the entire cavity floor, which yields much lower resistivity values than those expected from the bedrock. The superficial layer (1 or 2 m thick) yielded a resistivity lower than $2000\Omega\text{m}$ while the bedrock yielded a much higher resistivity (around $3000\text{--}7000\Omega\text{m}$). Although there were some gaps in the resistivity continuity of the bedrock, some of which are difficult to interpret, the study of Beltrami quarry was particularly easy due to the strong resistivity gradients between the two materials under investigation.

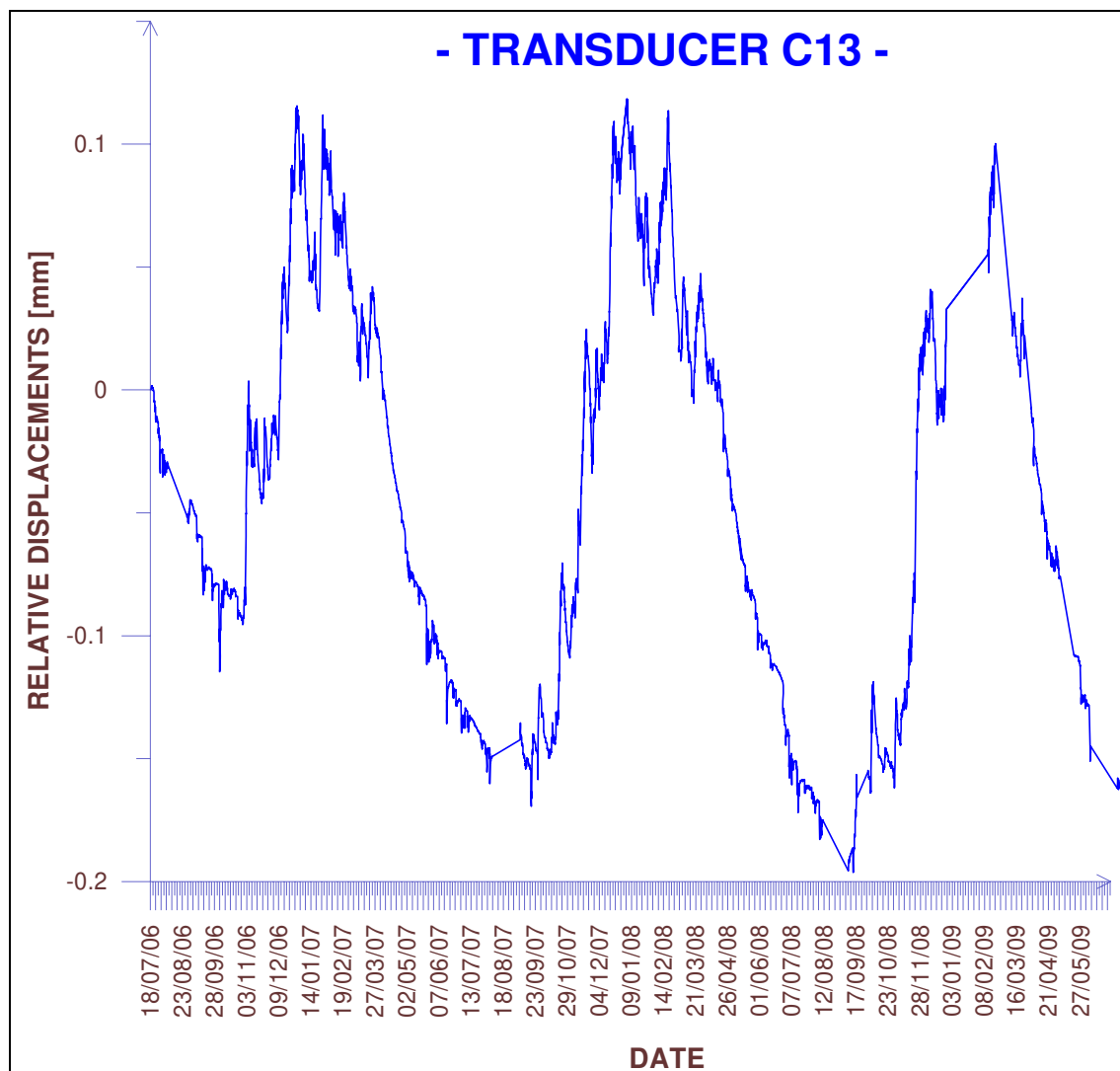


Figure 8. Readings from C13 transducer in period July 2006–May 2009.

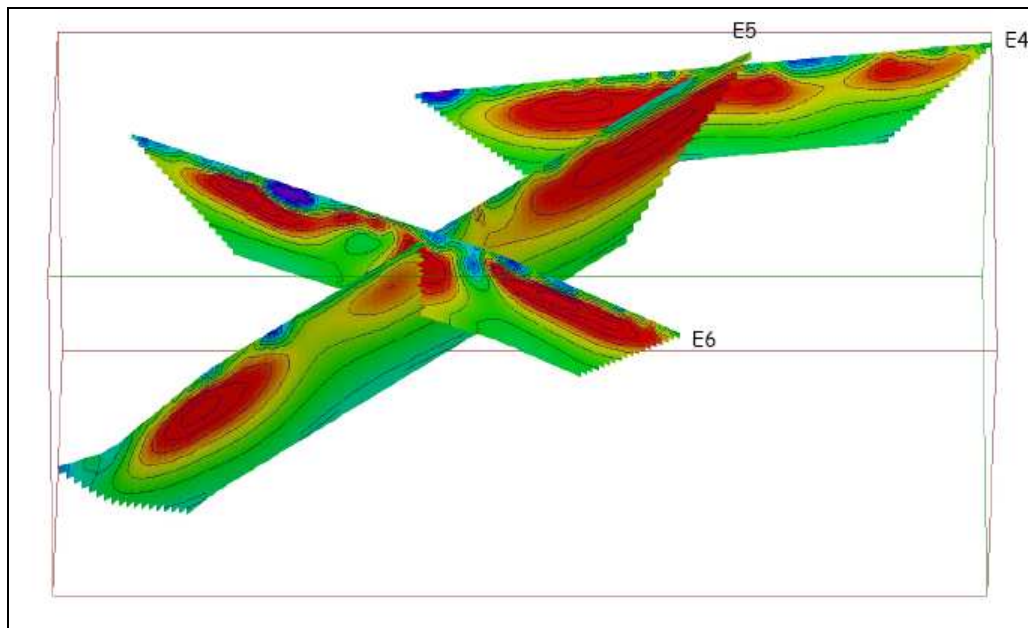


Figure 9. 3D tomographic section of quarry floor. See Figure 6 for positions of tomography lines.

Flat Jack Tests

The test locations were selected to obtain the most complete and exhaustive picture of the global stress state of the rock mass and of the local stress acting on the quarry site. A total of 13 single flat jack tests (ASTM D 4729-87, 1993) and three double flat jack tests were carried out. The single flat jack tests were based on the measurements of the displacements induced by the stress release around a flat cut normal to the investigated direction. The stress release induces, in the case of a compressive state of stress, a closure of the cut which can be measured by means of convergence measures between couples of points located symmetrically along the cut. This convergence can be eliminated by the introduction and subsequent pressurization of an appropriate flat jack. This procedure restores the local state of stress and allows for its measurement within the investigated area. The flat jacks used are of semicircular–elliptical shape with a nominal surface of 778 cm². The flat jack is made of two sheets of metal welded along their boundaries (the total thickness of a flat jack is 3.5 mm). Two metallic pipes welded along the straight edge of the jack allow a connection with the pressurizing units; each single part of the instrument (metal sheets, weldings, pipes) is tested at high pressure to verify a seal is maintained under test conditions. The convergence was tested by means of a removable mechanical caliper with a sensitivity of 0.001 mm on a measurement basis of 100 mm length. The measurement points are materialized by gluing 5-mm brass disks to the rock mass. The measurement of the applied pressures is carried out using two manometers, one connected to the pump and the other to the flat jack pipes. The flat jack technique was used to determine the vertical state of stress on some pillars and underground opening walls.

Nine tests were performed on the pillars (see Figure 7 for location of the pillars) and the boundary walls by allowing the estimation of the acting state of stresses (see Table 6). These results were then used for the numerical model calibration.

Table 6. Results obtained from flat jack test in pillars and boundary walls (FON).

Location	Measured stress (MPa)
Pillar 13	1.74
Pillar 23	2.14
Pillar 40	0.0
Pillar 54	5.00
Pillar 63M	2.16
Pillar 63V	0.00
Pillar 63M	5.57
FON 1–3	2.02
FON 2–4	7.68



STABILITY ANALYSIS

The stability analysis was carried out using different approaches and considering the rock mass as a continuous and a discontinuous media depending on the scale of the problem and on the aspect being analyzed. Both local and global stability conditions have been investigated. Local conditions are mainly governed by preexisting discontinuity while global stability is a result of the iteration between rock mass strength and induced stress. The key block (KB) method has been applied for the stability analysis of the underground access areas where block detachment from the roof and from the walls was observed. The global stability was studied using 3D FEM modeling of the whole excavation. The FEM results were calibrated by comparing them with flat jack results while the KB results were compared with in situ observation of unstable blocks.

KB Analysis at Danzi Quarry

This area, characterized by a high fracture density, was carefully surveyed in order to identify the presence of joint sets and their main features (see Tables 3 and 4). Stability analyses of the three entrances have been treated separately, considering the discontinuities surveyed in correspondence with the different accesses. A stability analysis was then performed by applying the Rock3D code (Geo&Soft, 2008), in implementing the KB method. Stability analyses were first carried out in a statistical way. In this case, the presence of 4- and 5-joint sets was considered to investigate the influence of different clustering schemes due to wide joint orientation dispersion. Subsequently, corresponding data measured at the three entrances have also been treated deterministically in order to determine the exact volume and location of unstable blocks.

The parametric analysis of the discontinuity shear strength has also been considered. Laboratory tests on discontinuities have shown shear friction angles of 51° and 41° , respectively, for peak and residual condition. However, in situ observations have outlined the presence of non-fully persistent discontinuity and weathering due to karst actions. These two effects caused the authors to take the cohesion value (due to rock bridges) and the low friction angles (due to karstic action) into account. The results obtained on the central entrance indicated that for friction angles below 44.5° , instability occurs for all finite and removable blocks. For friction in the range of 30.3° – 32.9° , the safety factor (SF) varies from 1–1.3 (see Figure 10).

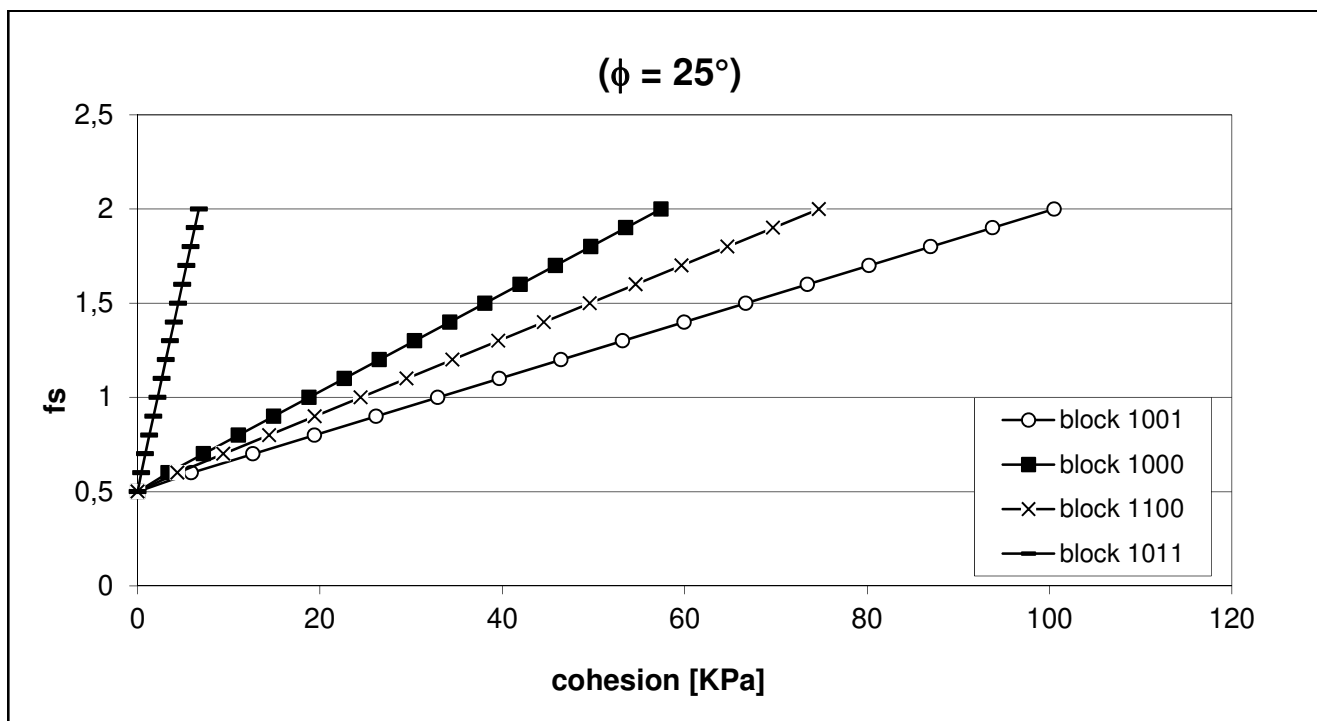


Figure 10a. Variation of SF with cohesion (friction angle = 25°).

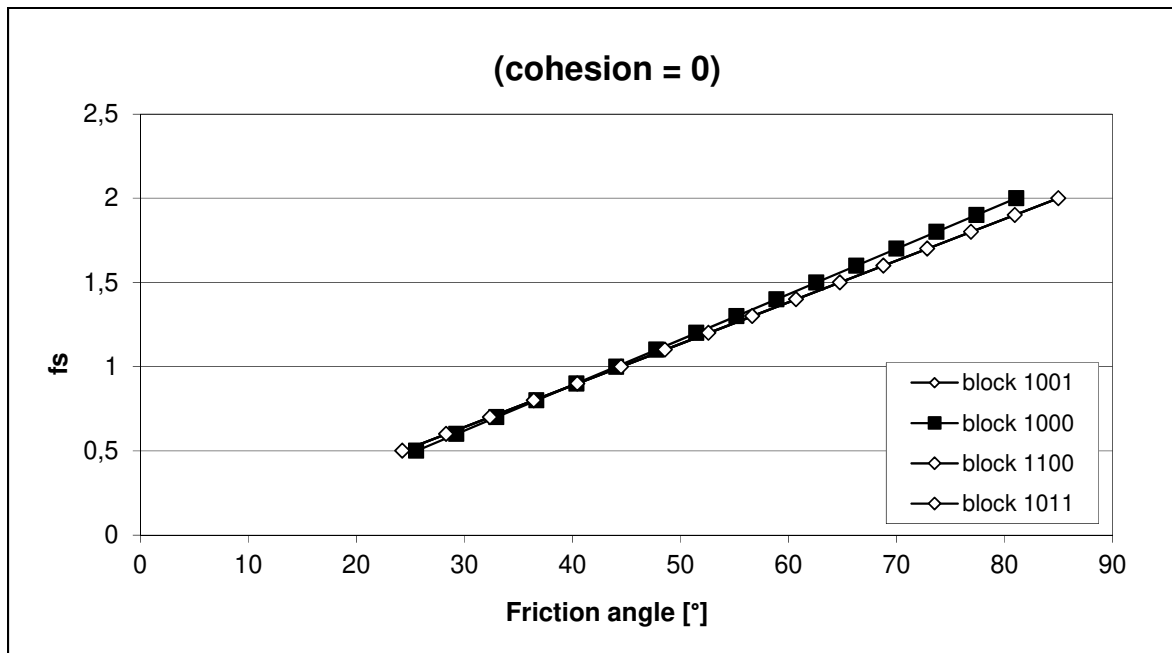


Figure 10b. Variation of safety factor (SF) with friction angle (cohesion = 0).

For friction angles above 56.6°, SF > 1.3. For the lower entrance, similar results have been obtained where instabilities occur at friction angles below 53.7°. All of the finite blocks are unstable at the upper entrance of the Danzi quarry. On the other hand, cohesion in the range of 20–30 kPa can guarantee stability for most blocks. Table 7 reports the results subdivided for each examined entrance area.

Table 7. Brief description of stability analysis of blocks in proximity of the quarry entrances.

Entrance studied	Unstable volume(m ³)	No. of blocks	Sliding direction	Type of sliding	SF
Lower 5 sets	2.837	1	A(56.65°/273.22°) B(87.97°/343.36°)	3D	<1
	4.429	1	B(87.97°/343.36°) C(62.41°/234.89°)	3D	<1
	0.047	1	A(56.65°/273.22°)	2D	<1
Lower 4 sets	5.178	1	F(56.65°/273.22°) I(87.97°/343.36°)	3D	<1
	1.105	1	F(56.65°/273.22°) I(87.97°/343.36°)	3D	<1
Central 5 sets	0.658	1	O(88°/300°) P(44.89°/225.44°)	3D	<1
	0.089	1	M(63.25°/243.51°) P(44.89°/225.44°)	3D	>1
Central 4 sets	11.865	1	R(55.62°/237.3°) O(88°/300°)	3D	<1
	0.003	1	R(55.62°/237.3°) O(88°/300°)	3D	<1
	2.207	1	R(55.62°/237.3°) O(88°/300°)	3D	<1
	4.849	1	R(55.62°/237.3°) O(88°/300°)	3D	<1
Upper 5 sets	15.194	1	V(78.53°/340.21°) Z(78°/240°)	3D	<1
	0.577	1	V(78.53°/340.21°)	2D	>1
	0.684	1	U(16.22°/197.29°) W(85.77°/286.31°)	3D	>1
	0.036	1	V(78.53°/340.21°) Z(78°/240°)	3D	<1
Upper 4 sets	0.004	1	A1(85.77°/286.31°) C1(78°/240°)	3D	<1
	0.109	1	C1(78°/240°)	2D	<1

On the basis of the obtained results, we could deduce that most of the finite and removable blocks are unstable when the discontinuities are fully persistent and weathered. Consequently, a reinforcement system such as bolting must be considered. Finally, the worst-case scenarios (in terms of instability and block volumes) were considered for the design of reinforcement systems.



KB Analysis at Beltrami Quarry

As for Danzi quarry, all the measured discontinuities have been considered and a statistical analysis was performed on the quarry roof, walls and pillars. Next, a deterministic analysis was performed on the entrance area by applying the real, observed discontinuities in their measured position. The challenge we faced was that discontinuities observed on the quarry roof were not directly accessible due to the height of the roof, so their traces could roughly indicate their dip direction but not their dip. A parametric analysis was then carried out by varying the orientation of each observed discontinuity according to the mean orientation of the three most representative joint sets.

Finally, the worst-case scenario (in terms of instability and block volumes) was considered. Discontinuity shear strength was applied with a friction angle of 25° and cohesion varying in the range of 0–300 kPa. Unstable blocks have been identified on both the quarry roof and walls. Seven blocks were found on the roof (see Table) in terms of average volume. The largest unstable block (No. 2) has a volume of 4.108 m^3 and is within 40 cm of the quarry entrance.

Table 8. Geometry of unstable blocks.

Block	Volume (m^3)	Side	Area (m^2)	Dip	Dip direction
1	2.110	2	0.218	76	25
2	4.108	2	0.701	76	25
		3	0.124	76	25
3	0.490				
4	1.870				
5	1.125	1	0.231	76	25
6	1.482	1	0.316	76	25
7	0.800	1	0.158	76	25

Concluding Remarks on KB Analysis

The results obtained confirm in situ observations that there are unstable blocks of variable volumes ($0.01\text{--}0.015 \text{ m}^3$) in both quarries. Larger blocks of some cubic meters are also present at the central entrance of Danzi quarry. KB computations have shown that blocks of different dimensions can detach from the quarry roofs since rock bridges can only guarantee their stability temporally. Since weathering phenomena are expected due to the karst nature of the rock mass, further stability support is needed for each finite and removable block.

3D NUMERICAL MODELING OF PILLARS

2D and 3D FEM models were used to study the global stability of the voids. First, 3D pillar models were set up and analyzed individually; then, the entire quarry was modeled.

Due to the old quarrying techniques (hammer and chisel) that were used to exploit the Viggiù ornamental stone, the shape of the pillars and the geometry of the entire quarry are irregular and the underground chambers were excavated with a strong dip following the useful sandstone layer. Such exploitation has resulted in pillars of irregular shape and geometry (see Figure 11a) and chamber floors and roofs inclined at around 30° (see Figure 12). Therefore, much time and effort has been expended on defining the geometry of the model. The use of specialized 3D CAD software has been necessary in order to reproduce the complex geometry of the pillars. The geometry has been subsequently exported to 3D FEM software for the analysis (see Figure 11b). The geometry of the pillars, of the entire quarry and of the territory surrounding it has been established from a detailed topographic survey that was carried out both within and outside of the quarry site.

The first analysis defined the most appropriate mechanical features of the rock mass using a back analysis procedure on the pillars where flat jack tests were performed. The comparison between numerical results and on-site outcomes allowed for an appropriate and reliable calibration of the numerical model and for use as a provisional tool. Particular care has been paid to the definition of the loading condition of the pillars. In a local model, such as the one reported in Figure 11, the correct definition of the loading condition is essential for a proper numerical calculation. The reported pillar is located inside the Beltrami quarry, has a height of approximately 7 m, is highly irregular and the rock overburden is around 13 m high. The area of influence of the pillar is around 200 m^2 . In order to calculate the load that should be applied to the pillar



roof, the total load of the rock overburden can be calculated by determining the total volume of rock between the quarry roof and the terrain surface above it (limited to the area of influence being considered).

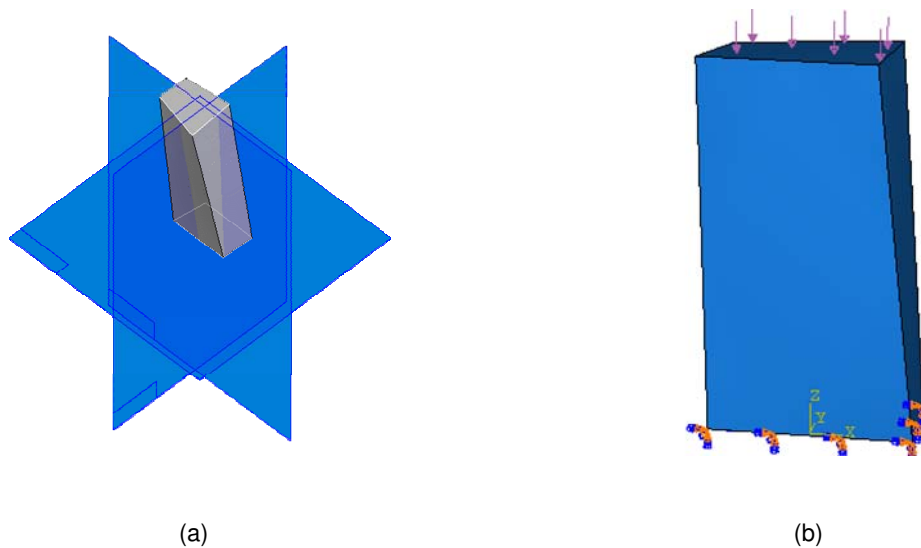


Figure 11. (a) View of pillar No. 23 (see Figure 7) as modeled with ABAQUS software (Hibbit, Karlsson and Sorensen, Inc., 1994); (b) different 3D view of same pillar with boundary conditions and applied loads.

However, results obtained using single pillars do not take into account the real geometry of the excavation that causes a variation in the stress acting on the pillar. In order to better allow for such an effect, 2D numerical models of the vertical sections have been created. The model containing pillar 23 (see Figure 7 for position) is shown in Figure 12a. The stress condition thus obtained was then used as a load for the 3D model of the pillar.

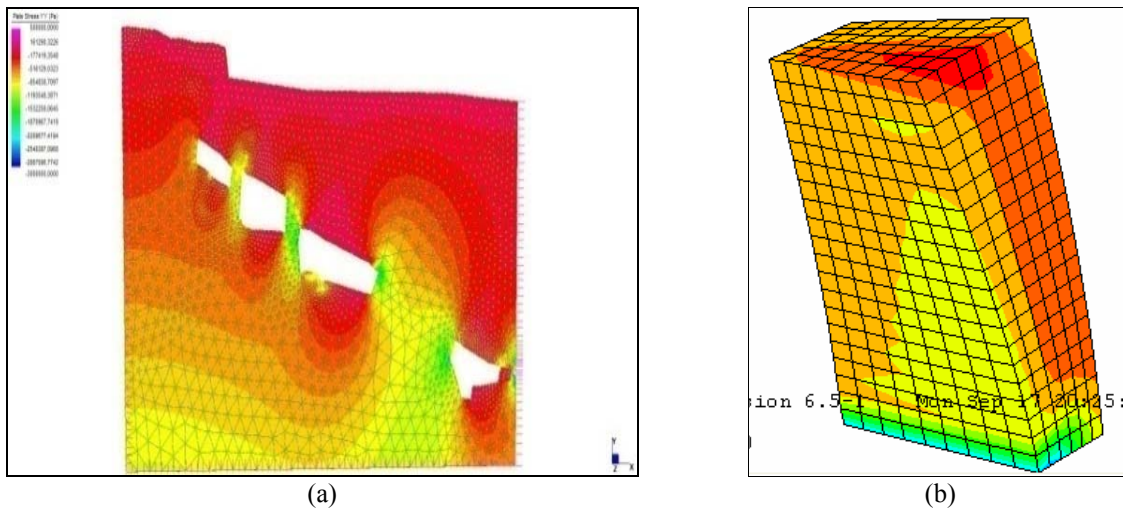


Figure 12. Vertical stresses: (a) 2D model of vertical section on pillar No. 23 (in center in (a)) modeled with Straus/ (G+D Computing, 1999) (see Figure 7 for pillar location on a map); (b) 3D model of pillar using ABAQUS code.

The FEM analysis on pillar 23 (see Figure 7) returned a value of approximately 2.22 MPa for vertical stress in the area where the flat jack test was performed, which fits well with the experimental results that indicate a vertical stress of 2.14 MPa. The same conceptual procedure has been used for all of the pillars and walls that were tested with the flat jack. The mechanical features of the rock mass after the calibration procedure are reported in Table 9.



Table 9. (a) Comparison between state of stress measured by flat jack tests and numerical model outcomes; (b) rock mass features considered in numerical model (see Figure 6 and 7 for location of pillars).

Location	Measured stresses (MPa)	Calculated stresses (MPa)	State	Mechanical features	Numerical values (Pa)
Pillar 13	1.74	2.08	Compression	Elastic modulus	7.83×10^9
Pillar 23	2.14	2.22	Compression	Poisson's ratio	0.35
Pillar 40	0.0	0.02	Unloaded	Density	2.7×10^3
Pillar 54	5.00	7.27	Compression	Non-linear type	Elastic plastic
Pillar 63M	2.16	3.7	Compression	Yield criterion	Mohr-Coulomb
Pillar 63V	0.00	0.01	Unloaded	Friction angle	35°
Pillar 65V	5.57	8.65	Compression	Cohesion	3.00×10^5

(a)

(b)

The results obtained from the numerical model of the analyzed pillars are compared to those obtained from the flat jack tests in Table 10. Once the model had been calibrated, the stability condition of the entire quarry was verified by analyzing the plasticity of the rock mass and verifying that the rock mass was still in an elastic condition in most of the excavated areas.

Pillar Safety Factors

The design of the rock structures to be preserved as support in a room and pillar mining exploitation is conventionally carried out by assessing the SF of individual pillars. The computation can be done using an empirical formulation which is able to evaluate the ratio between the assessed pillar strength and the acting pressure. The pressure acting on a pillar is usually evaluated by the tributary area method (Brady and Brown, 2004).

Since the FEM method allowed us to compute the vertical stresses in every FEM mesh element, we were able to evaluate the acting pressure by calculating the average vertical stress in the middle section of each pillar rather than by using the area tributary method.

The pillar strength was evaluated using the formula proposed by Hedley and Grant (1972):

$$S_p = S_0 \cdot \frac{a_p^{0.5}}{h_p^{0.75}} \quad (1)$$

where:

S_p is the pillar strength,

S_0 is the uniaxial compression strength of rock mass,

a_p is the length of the pillar and

h_p is the height of the pillar.

Table 10. Comparison of measured vs. numerically predicted vertical stress on pillars

Location	Flat jack tests (MPa)	3D numerical model(MPa)	State
Pillar 13	1.74	1.70	Compression
Pillar 23	2.14	2.46	Compression
Pillar 40	0.0	0.7	Compression
Pillar 54	5.00	2.0	Compression
Pillar 63M	2.16	2.28	Compression
Pillar 63V	0.00	1.00	Compression
FON 1-3	2.02	1.9	Compression
FON 2-4	7.68	1.9	Compression



According to suggestions by Sheory and Singh (1974), S_0 was assessed by taking the Bieniawski (Bieniawski, 1973) RMR index into account as follows:

$$S_0 = \sigma_c \cdot e^{\frac{RMR - 100}{20}} \quad (2)$$

Where σ_c is the intact rock uniaxial strength. In the examined case σ_c is, on average, equal to 110 MPa; consequently, $S_0 = 13.47$. Therefore, the safety factor gives $F = S_0/\text{average } v_v$.

Table 11 reports a few values of the SF that were computed in pillars where flat jack measurements were performed. The comparison between the measured vertical stresses (from the flat jack tests) and the averaged computed vertical stresses (from the numerical model) indicates how the flat jack measurement are not reliable when, such in this case, the single pillar is subjected to flexural compression.

Table 11. Comparison of computed stress by FEM models and pillar resistance.

Pillar number	S_p (MPa)	Safety factor (SF)
Pillar 13	5.72	3.38
Pillar 23	4.20	2.80
Pillar 40	5.43	4.52
Pillar 54	4.46	4.02
Pillar 63M	5.86	4.54
Pillar 63V	5.86	4.54
Pillar 65M	4.41	2.14

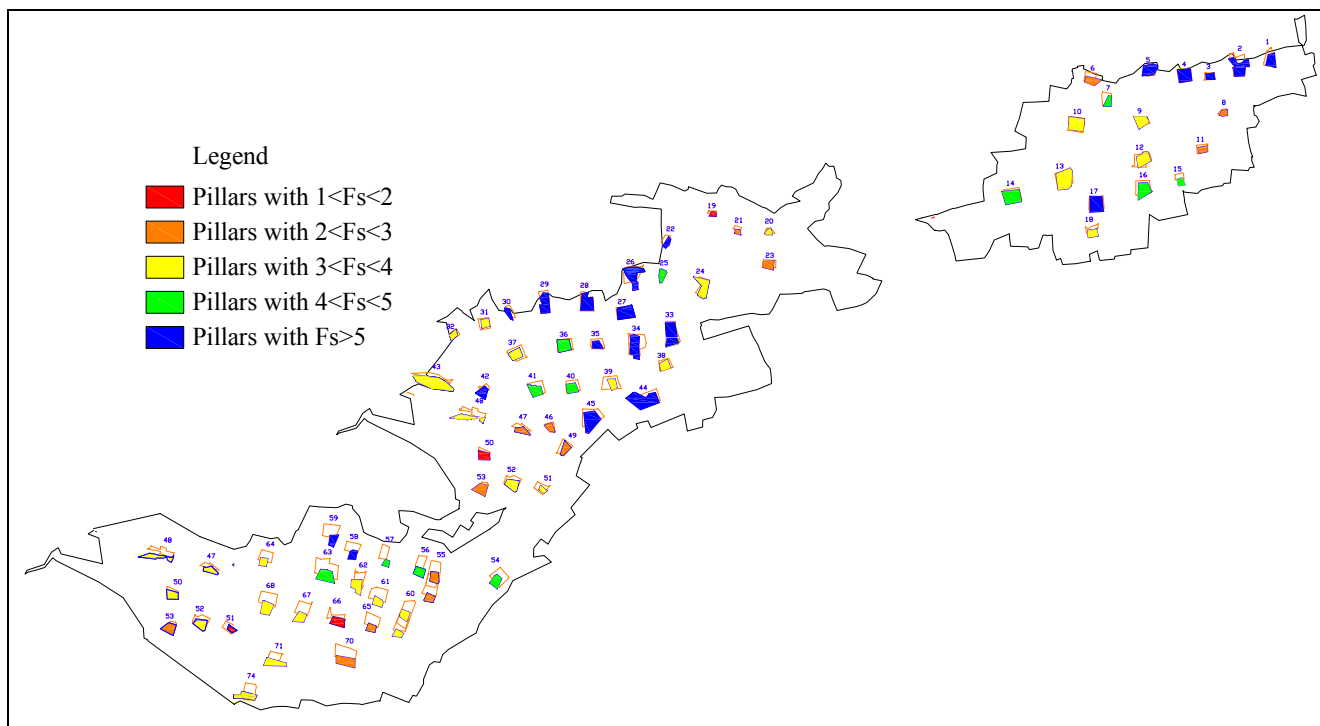


Figure 13. Quarry map reporting SF range for each pillar.

Figure 13 shows the SF computation for each pillar in the entire quarry. This graphical representation has been used to identify an optimal route for visitors in light of the stability of the various pillars.



REINFORCEMENT WORKS

Design of System

Reinforcement design was carried out according to the block reinforcement procedure (BRP) (Oreste and Cravero, 2008). This method was developed for passive bolting dimensioning for rock block reinforcement. The method can be applied to blocks of small to medium dimensions that are possibly detaching from vertical walls or from roofs. The computation method considers the response of the bolt through the unstable block. The unknowns of the method are: axial forces and shear and flexural forces along the bolt caused by small displacements due to the unstable block. According to this procedure, the correct bolt can be obtained after a series of tests using a trial and error method which compares different bolting schemes. The factors of safety obtained in the different scenarios are compared until the required safety conditions are reached. Finally, the required stabilization force is determined.

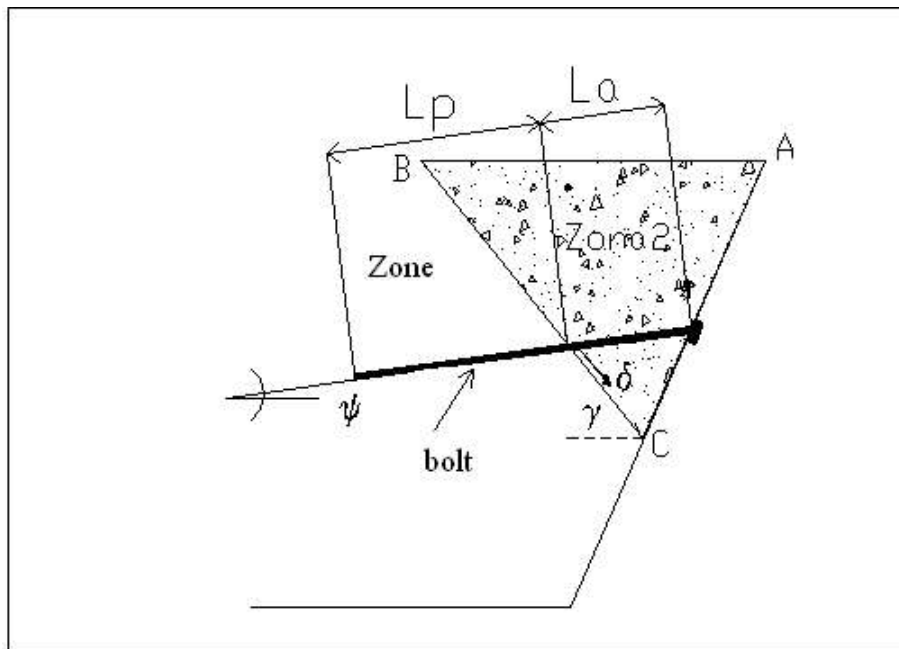


Figure 14. Scheme of interaction between rock mass and bolt; L_a : length of bolt in unstable zone (zone 1); L_p : length of bolt in stable zone (zone 2); δ : block displacement along sliding; ψ : dip of bolt from horizontal plane; γ : angle between sliding direction and horizontal plane.

For an easier application of the method, a Matlab code was developed. The bolt orientation (bolt trend and plunge) is used as the input data for the code. Since in this case the system has been applied to the roof reinforcement, vertical bolts have been considered for all blocks. Block displacement directions were obtained directly from the Rock3D numerical code.

The bolt chosen for this application is 3 m in length and the maximum bolt length inside the rock block computed by Rock3D is 1 m. The number of bolts changes for each block as a consequence of the dimensions of the block. The hole diameters are a consequence of the bolt type that is chosen. The properties of the bolt steel and of the cement mortar utilized for bolt installation are obtained from the commercial data.

Shear deformability at the rock mortar contact and at the bolt–mortar contact can be obtained at this design phase; based on previous research, we know that and depends on the rock and the mortar type. The minimum accepted factor of safety is also chosen. Code output is the stabilization force generated for each analyzed block grid and the global block weight. The SF of the stabilized block is computed by the code as the ratio between the stabilizing force and the acting forces.

Shear deformability at the rock mortar contact and at the bolt–mortar contact can be obtained at this design phase; based on previous research, we know that and depends on the rock and the mortar type. The minimum accepted factor of safety is also chosen. Code output is the stabilization force generated for each analyzed block grid and the global block weight. The



SF of the stabilized block is computed by the code as the ratio between the stabilizing force and the acting forces.

Table 12 reports the input data for two of the examined blocks (c26 and e40) and the results. Several different types of bolt are available on the market. In order to select the most appropriate bolt, one must consider the environmental conditions and the type of rock mass involved.

DESIGN AND VERIFICATION OF PATH FOR VISITORS

Since July 2003 the area of Mt. San Giorgio, of which the quarry site is an important part, has been included in the UNESCO World Heritage List. This decision was made by the UNESCO International Committee after an uncommonly fast administrative procedure, which endorsed the exceptional value of the site. The particular importance of Mt. San Giorgio is related to the presence of exclusive paleontological findings in the area. Since the second half of the 18th century when research studies initiated, thousands of reptile and fish fossils have been discovered—some of which belong to extremely rare or unique species.

Table 12. Bolt design on basis of BRP method (Oreste and Cravero, 2008) of two representative blocks.

	Block c26	Block e40
Volume	1.175 m ³	1.375 m ³
Weight	0.0317 MN	0.0317 MN
Borehole diameter	38 mm	38 mm
Bolt diameter (full section iron bar)	16 mm	16 mm
Total length of bolt	3 m	3 m
Foundation length	1 m	1 m
Orientation angles of block displacement vector	260/65	350/88
Total resultant (2 bolts per m ²)	0.0615 MN	0.0637 MN
R	1.94	1.71

The UNESCO accreditation supports the recovery of this cultural and scientific heritage and its development as a cultural, educational and tourist site that goes beyond local geographical interest. Part of the overall recovery project will be devoted to the design and verification of an appropriate route for visitors that would allow the public access to the underground quarries, beginning from the lower entrance to Danzi quarry and ending at the upper entrance to Beltrami quarry.

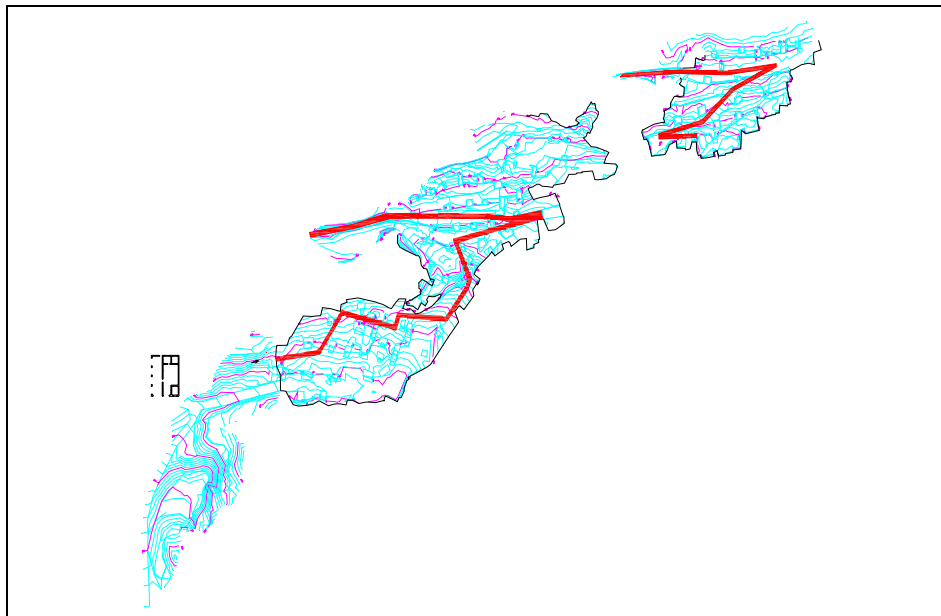


Figure 15. Map showing route for visitors (red) inside underground quarries.



The path starts from the most recently excavated chamber, where the material was excavated using the diamond wire technique and some majestic pillars were left in place to guarantee the overall stability of the quarry. These pillars became one of the particular features of these quarries. The first chamber is also characterized by the presence of old mining tools, diamond wire cutting machines and a number of buildings that were used as warehouses and workshops by the miners.

The route continues underneath a “mining well” that was used to collect and dispose of the mining debris. The well borders two majestic pillars that, due to the excavation of their upper part for further material recovery, stand in an atypical U shape. The route to the upper chamber includes the climb up a stairway made of stones. This excavation chamber is brighter thanks to the light that filters in from the north entrances. In this area the large artificial tank, recovered inside the rock mass as a reservoir for the mining operation, constitutes the main element of interest along with some impressive supporting walls that were used to terrace the filling debris.

A short distance outside the quarries (see Figure 16), visitors walk between several ancient stone walls inside a well-kept forest and then reach the entrance to Beltrami quarry. This quarry is the oldest and was excavated using the manual hammer-and-chisel technique. Traces of such activity can be seen along the walls and on the sides of the pillars.

A picturesque element is added by the black signs left on the roof of the excavations by the burning acetylene lamps. Inside the single chamber of the quarry, a visitor winds between the pillars and follows the old track that the miners walked every day to reach their work areas. This track was built by the miners themselves, using the debris from the quarry for raw material. The track concludes at the end of the chamber, where the old technique used for material removal can be admired from a few blocks that were left in place when the quarries were abandoned. The total length of the track is about 600 m and the total height difference is 100 m. The visit is especially safe and does not require any particular physical training.

CONCLUSIONS

The observations and results obtained from this monitoring system are of up most importance for understanding the behavior of the rock mass and calibrating the numerical modeling phase.

Both discontinuous and continuous schemes have been adopted to interpret the behavior of the rock mass around the excavation voids. Selected joints, considered in relation to the seasonal rainfall and temperature variations, were used to analyze block behavior. Flat jack results were utilized to set up a FEM numerical analysis, which considered the rock mass as an equivalent continuum.

The rock mass was modeled by FEM at different scales (at the pillar scale in 3D and in 2D models in several vertical sections) in order to determine the actual load acting on the pillars. After calibrating the model by comparing its results with the flat jack results, a stability analysis of the pillars was performed by analyzing the induced state of stress. All the pillars are strongly inflected due to their geometrical shape. Thus, the stress distribution is strongly inhomogeneous. Most pillars show a side with high compressive load, but are still in the elastic region and another side that is nearly uncharged but still in compression. Consequently, the stability of the pillars can be assessed in all cases where preexisting discontinuities are not crossing the pillars.

Discontinuous analyses were carried out by applying KB theory on the quarry entrance, roofs, walls and pillars. Several possibly unstable blocks have been identified deterministically. In these cases, a specific reinforcement system based on the installation of a net of rock bolts was calculated. The calculation was carried out using the BRP method (Oreste and Cravero, 2008).

The monitoring system has demonstrated its fundamental role and, consequently, must be maintained for the time being in order to allow for a complete and global analysis of the displacement behavior of the rock mass during several seasonal cycles. For this purpose, a system for the automatic numerical analysis of the monitoring results and for their integration with meteorological, climatic and seismic data is under development. Once completed, the system will allow for a prompt update of the FEM model, which will quickly evaluate the response (in terms of stability and stress-strain behavior) of the rock mass to the new boundary conditions. This study is intended to be a primary phase of a wider analysis of the general geomechanical condition of this complex of quarries that has a final objective of defining the stability of the entire rock mass containing the Viggù quarries.

The preliminary design of the path for visitors aims to valorize and protect the local historical and cultural heritage and is



well in agreement with the purpose of the UNESCO International Committee. These quarries are a wonderful example of archeological mining and are testimony to ancient mining techniques and to the lifestyle connected with the old ornamental stone industry. Another fundamental aspect that should not be underestimated is the beauty and uniqueness of the site, the majesty of the mining chambers and the large size of the pillars that, filtering the limited sunlight, are creating picturesque and changing scenarios inside the underground structures. Finally, the UNESCO accreditation is a perfect platform on which to start the restoration of this unique environment that has been neglected for such a long time.

The proposed route has been determined on the basis of historical and environmental interests. The hazard map, determined on the basis of results from the stability analysis, was superimposed over the proposed path to determine the reinforcement works needed in the different areas of the quarries.

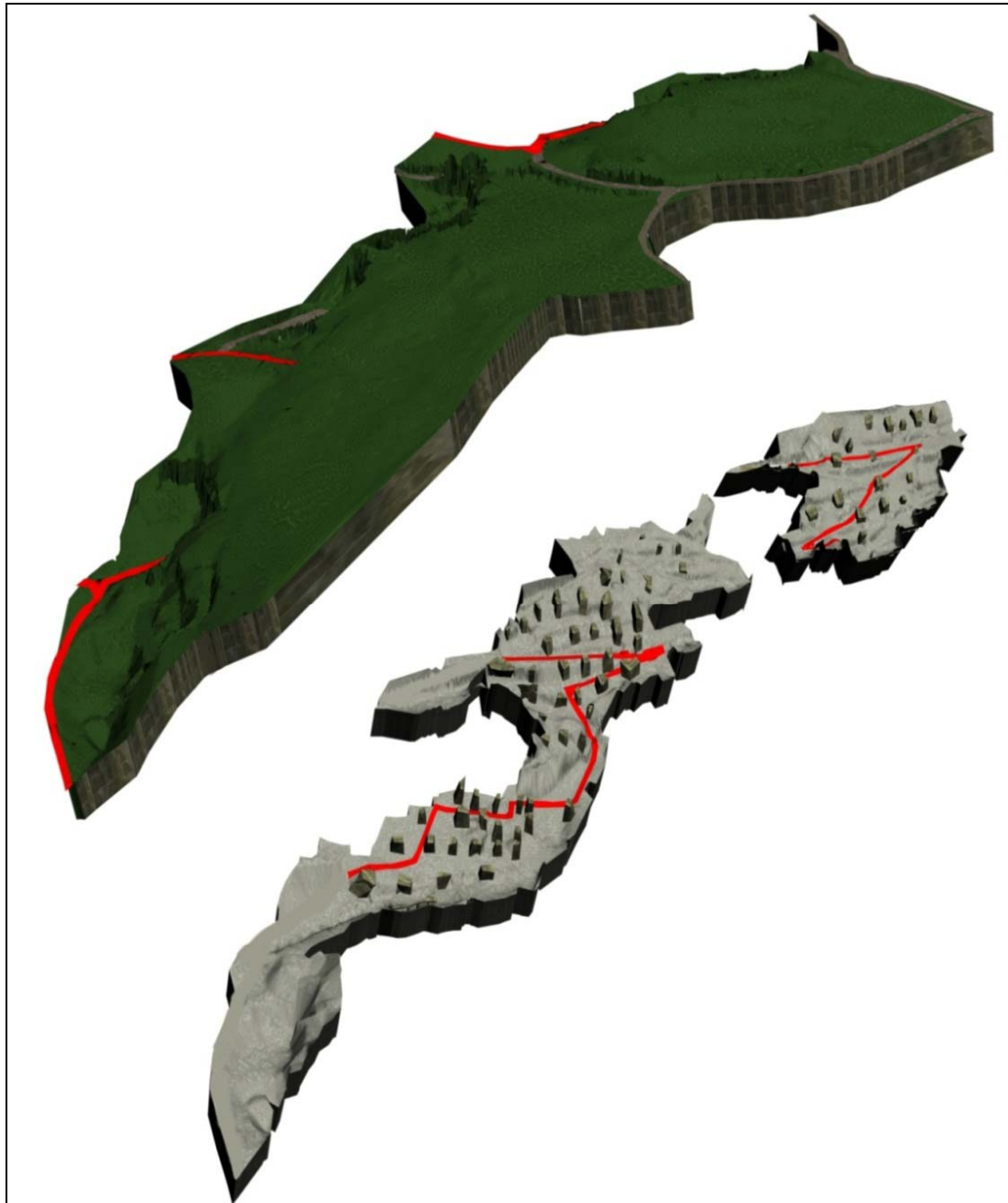


Figure 16. 3D rendering of route for visitors. External area (above) and underground path (below).



REFERENCES

- ASTM D 4729-87. (1993). "Standard test method for in-situ stress and modulus of deformation using the flatjack method." 1993 Annual Book of ASTM Standards, Vol. 04-08.
- Barton, N., Lien, R., and Lunde, J. (1974). "Engineering Classification of Rock Masses for Design of Tunnel Support." Rock Mechanics, pp. 186–236.
- Bieniawski, Z.T. (1973). "Engineering classification of jointed rock masses." Transaction, South Africa Institution of Civil Engineers, pp. 335–344.
- Brady, B.H. and Brown, E.T. (2004). Rock Mechanics for Underground Mining. London: Kluwer Academic Publisher.
- G+D Computing. (1999). "Straus7. Using Strand7 User Manual". Sydney, NSW 2000, Australia, May 1999.
- GEI Elettronica. (2005). "Sms Manager. Sms Manager User Manual." Parma, Italy.
- Geo&Soft. (2008). "Key block theory based three dimensional rock block analysis. Rock3D. Manual." Tratto da Geo&Soft: <http://www.geoandsoft.com>.
- Hedley, D., and Grant, F. (1972). "Stope-and-pillar design for the Elliot Lake Uranium Mines." Bulletin of Canadian Institute of Mining Metallurgy, pp. 37and 44.
- Hibbit, Karlsson and Sorensen, Inc. (1994). "Abaqus Standard." Pawtucket, RI, USA.
- Hoek, E., and Brown, E. (1997). "Practical estimate of rock masses." International Journal of Rock Mechanics and Mining Sciences, pp. 1165–1186.
- Hoek, E., Carranza T.C., and Corkum, B. (2002). Rocscience. From Rocklab freeware software: <http://www.rocscience.com>.
- Oreste, P., and Cravero, M. (2008). "An analysis of the action of the stabilization of rock blocks on underground excavation walls." Rock Mechanics and Rock Engineering, Vol. 41, pp. 835–868.
- Palmström, A. (1995). Ph.D. Thesis. "RMi - A rock mass characterization system for rock engineering purposes." Norway.
- Rocscience Inc. (2007). RocLabUser's Guide. Toronto, Ontario, Canada.
- Scesi, L. (2000). "Studio geologico, idrogeologico e geologitotecnico delle antiche cave sotterranee di pietra di Viggiù, Saltrio e Brenno." Milano: Politecnico di Milano.
- Sheory, P., and Singh, B. (1974). "Estimation of pillar loads in single and continuous seam workings." International Journal of Rock Mechanics and Mining Sciences, pp. 97–102.



INTERNATIONAL JOURNAL OF GEOENGINEERING CASE HISTORIES

*The Journal's Open Access Mission is
generously supported by the following Organizations:*



Access the content of the *ISSMGE International Journal of Geoengineering Case Histories* at:
www.geocasehistoriesjournal.org